Elsevier Editorial System(tm) for Bioresource Technology
Manuscript Draft

Manuscript Number: BITE-D-19-07665R1

Title: Aeration control in Membrane Bioreactor for sustainable environmental footprint

Article Type: VSI:BNR

Keywords: membrane bioreactor, aeration-based control strategy, proportion-integration control

Corresponding Author: Professor Giorgio Mannina, PhD

Corresponding Author's Institution: Università di Palermo

First Author: Giorgio Mannina, PhD

Order of Authors: Giorgio Mannina, PhD; Alida COSENZA; Taise Reboucas

Abstract: Aeration in membrane bioreactor systems for wastewater treatment is one of the main source for energy consumption. In this study different scenarios were scrutinized to minimize the energy consumption. Specifically, open-loop and closed-loop scenarios were performed by a two-step cascade control strategies based on dissolved oxygen, ammonia and nitrite concentrations. An integrated MBR model was employed which includes the greenhouse gas formation/emission processes. The air flow in closed-loop control led to a substantial reduction in terms of energy consumption (32% for Scenario 1 and 82% for Scenario 2). The air flow control based on both ammonia and nitrite concentrations within the aerobic reactor (Scenario 2) provided excellent results in terms of operating cost (64% reduction), direct (10% reduction) and indirect (81% reduction) emissions.

*Highlights (for review)

Highlights

- Two-step cascade control strategies have been applied to MBR
- An integrated MBR mathematical model has been adopted
- Energy consumption reduces till to 82% controlling the aerobic airflow rate
- Operating cost reduces till 64 % controlling the aerobic airflow rate
- Direct GHG emission reduces from 0.52 to 0.47 kgCO_{2eq} m^{-3} under control condition

Aeration control in Membrane Bioreactor for sustainable environmental footprint

Giorgio MANNINA[1,2*], Alida COSENZA[1] and Taise Ferreira REBOUÇAS[1]

[1]Engineering Department, Viale delle Scienze, Ed.8, 90128, Palermo, Italy

[2]College of Environmental Science and Engineering, Tongji University, 1239 Siping Road, Yangpu District, Shanghai, 200092, China

*Corresponding author: giorgio.mannina@unipa.it, tel. +3909123896556

Abstract

In this study different scenarios were scrutinized to minimize the energy consumption of a membrane bioreactor system for wastewater treatment. Open-loop and closed-loop scenarios were investigated by two-step cascade control strategies based on dissolved oxygen, ammonia and nitrite concentrations. An integrated MBR model which includes also the greenhouse gas formation/emission processes was applied. A substantial energy consumption reduction was obtained for the closed-loop scenarios (32% for Scenario 1 and 82% for Scenario 2). The air flow control based on both ammonia and nitrite concentrations within the aerobic reactor (Scenario 2) provided excellent results in terms of reduction of operating cost reduction (64%), direct (10%) and indirect (81%) emissions.

Keywords: membrane bioreactor, aeration-based control strategy, proportion-integration control.

1. Introduction

Wastewater treatment plants (WWTPs) can be responsible for both liquid and gaseous pollutants discharge into the environment. WWTPs operation has a constant challenge to provide the excellent effluent quality at the lowest operational costs as possible (Bozkurt et al., 2016). WWTPs are responsible for emitting almost 3% of the main greenhouse gases (GHG) (carbon dioxide - CO_2, methane - CH_4, and nitrous oxide - N_2O) by direct (due to biomass metabolism) and indirect (due to electricity and chemical consumption) sources (Mannina et al., 2016; Polruang et al., 2018; Koutsou et al., 2018; Domingo-Félez and Smets, 2020). Among the most relevant current challenges for WWTPs, GHG emission minimization is one of the utmost (Flores-Alsina et al., 2011).

In view of addressing the aforementioned challenges new operating strategies aimed at improving the overall WWTP performance are required (Wu et al., 2020). With this regard, the use of membrane bioreactors (MBRs) was introduced in the past decade, as a promising alternative to conventional activated systems (CAS) in order to obtain excellent effluent quality (Xiao et al., 2014; Liu et al., 2018). Indeed, MBRs are known due to their ability to provide high effluent quality, to reduce sludge production and to require low space for implementation (Guo et al., 2012). Despite the MBR advantages, their higher energy demand when compared to CAS (for membrane aeration, permeate extraction, among others) coupled with membrane fouling issues still represent serious drawbacks for the technology spread (She et al., 2016). With this regard, several efforts have been performed in literature in order to reduce MBR energy costs and to avoid/reduce/mitigate membrane fouling. Even though, literature is still far from finding a definitive solution for these issues (Krzeminski et al., 2017).

The high energy requirement of MBR represents an environmental issue since electricity is also related to GHG indirect emissions (Mannina et al., 2018a). A great part of the energy consumption in MBRs regards the presence of additional aeration systems for fouling mitigation and the presence of the permeate extraction pumps (Yang et al., 2016; Zheng et al., 2018; Zhang et al., 2019). The aeration systems are responsible for about 70 to 80% of the total energy consumption of a WWTP contributing substantially to the total plant operating costs (Sun et al., 2016; Xiao et al., 2014). Indeed, about 30% of the WWTP budget is related with the aeration systems (Metcalf & Eddy, 2003). For this reason, the optimization of aeration systems is imperative in view of reducing operating costs.

Aeration-based control strategies are reported in the literature with the attempt to optimize aeration systems by regulating the air blowers with the use of manual or automatic controllers (Maere et al., 2011; Sun et al., 2016). Nowadays, manual controllers are hardly implemented because they are susceptible to human errors. Thus, automatic controllers are preferable in order to ensure the optimal system response. However, the implementation of automatic aeration controllers in real WWTPs requires huge capital investments (Olsson and Newell, 1999), which makes the mathematical modelling a recommendable tool prior to the system's on-site installation (Rivas et al., 2008; Gabarrón et al., 2015). As a matter of a fact, model simulation enables decision-makers to act faster at the smallest disturbance, which constitutes one of the main reason that aeration control strategies are very often coupled with modeling systems (González et al., 2018). This coupling allows to compare and investigate several operational scenarios that are influenced by changes in aeration (Maere et al., 2011).

Most of the aeration-based control strategies are based on the real-time behavior of key process parameters, such as dissolved oxygen (DO) and ammonia (NH_4) concentrations. The purpose of a DO-based control strategy is to drive the DO concentration within the aerobic tanks towards a stable and optimized condition, in which the whole amount of air insufflated is sufficient for maintaining the biomass survival and the treatment process (Gabarrón et al., 2015). However, the DO concentration is an operational parameter that may influence several processes (e.g., nitrification and denitrification, biomass survival, GHG emissions); therefore, establishing a control strategy based only on the above aspect does not guarantee that the effluent quality respects the effluent standards (Wahab et al., 2009). For this reason, feedback control, which is based on ammonia concentration, is proposed in the literature with the aim of obtaining the optimal trade-off between the air supplied and the effluent quality (Wahab et al., 2009; Sun et al., 2016).

Two main control strategies are reported in the literature with the aim to optimize the air flow rate inside an aerobic compartment: i. open-loop control; ii. closed-loop control (Olsson and Newell, 1999). In the open-loop control, no automatic feedback derived from the real-time measurement is applied since the control is based on a timer and/or a predefined program of actions (e.g., time-set air supply in the aerobic reactor or

MBR) without looking to the effluent quality or gaseous emissions. On the other hand, in the closed-loop control, the actions (feedback) are automatic and based on real-time measurements (e.g., the control of the air flow rate inside the aerobic reactor is based on effluent ammonia concentration).

The open-loop control does not guarantee to meet the effluent limits of the discarged pollutants; indeed, not inter-related changes in the air supply, as a function of the effluent limits, will result in worsening/improving the WWTP performance in terms of carbon and nutrients removal (Kalboussi et al, 2018). Reagrding closed-loop control, literature reports some applications to MBR mainly focused on the optimization of the membrane filtration process (Ferrero et al., 2012). Specifically, Ferrero et al. (2011) applied a performance-based control to optimize aeration in MBR by using permeability as the key parameter. Results demonstrated that the reduction of the permeate flux can save up to 21% of the energy used for membrane aeration. Dalmau et al. (2014) applied an experimental approach based on establishing a DO setpoint to maintain aerobic conditions and lowering fouling in an MBR. Results indicated 75% of energy consumption reduction, without compromising nutrient removal efficiency. Sun et al. (2016) proposed an in-situ ammonia-based feedback control strategy to a full-scale MBR obtaining a reduction of the overall energy specific consumption up to 0.45kWh m^{-3} of treated effluent.

Some authors have also focused the attention on control/optimization strategies aimed at reducing the plant operational costs in anaerobic membrane bioreactors (AnMBRs), where the closed-loop control strategies are required for reducing membrane fouling and operating costs (Robles et al., 2018). Specifically, Benyahia et al. (2013) developed a model applied to an AnMBR with the aim to establish a control tool. In particular, Benyahia et al. (2013) focused the attention on the reduction of membrane fouling by controlling the soluble microbial products (SMP) formation/degradation process. Robles et al. (2014) applied an advanced knowledge-based control system aimed at optimizing the filtration process in an AnMBRs. The authors obtained substantial saving in energy requirements and operating costs (up to 25% and 53.3%, respectively).

Despite the above referenced literature studies, as far as the authors are aware, there is any study on the application of aeration/feedback control for MBR systems including multiple output variables: direct and indirect GHG emissions and effluent quality. This study presents a first attempt to apply a cascade control for an MBR systems by considerying a comprehensive analysis based on the above mentioned multiple outputs. The final aim of this study is to evaluate the effectiveness of feedback closed-loop strategies applied to an MBR pilot-plant focusing on system optimization in terms of effluent quality (gaseous and liquid), operating costs and energy consumption. With this regard, feedback closed-loop strategies were implemented by adopting an integrated MBR model (Mannina et al., 2018a-b). In particular, three scenarios are analyzed: i. Scenario 0 – reference scenario with open-loop control – air flow rate was optimized without considering any real-time measurement (Mannina et al., 2019); ii. Scenario 1 – with a closed-loop control where the aeration control is based on ammonia concentration inside the aerobic reactor; ii. Scenario 2 – with a closed-loop control where the aeration control is based on both ammonia and nitrite (NO_2) concentration inside the aerobic reactor.

2. Material and methods

2.1 The mathematical model

The integrated mathematical model applied here is characterized by two mai sub-models: biological and physical (Mannina et al., 2018b). The biological sub-model is based on the ASM2d algorithms proposed by Henze et al (2000) modified to include soluble microbial products (SMP) formation/degradation, GHG production/emission and detailed nitrogen transformation processes. More in detail, the biological sub-model consists of 116 parameters and 25 state variables. Nitrogen transformation is described as a two-step nitrification process (Pocquet et al., 2016) and four-step denitrification processes (Hyatt and Grady, 2008). The two-step nitrification considered by the sub-model is summarized as follows:

- First step: (i) NH_4 is oxidized into NO_2 by means of ammonia-oxidizing bacteria (AOB); (ii) incomplete ammonia oxidation may lead to the formation of intermediate products, such as hydroxylamine (NH_2OH) and nitric oxide (NO); (iii) oxidation of NH_2OH to NO_2, with the accumulation of NO; (iv) a reduction of NO may be observed leading to the formation of N_2O.
- Second step: the NO_2 is oxidized into nitrate (NO_3) by means of nitrite-oxidizing bacteria (NOB).

The four-step denitrification is assessed taking the contribution of the phosphorus accumulating organisms (PAOs) and heterotrophic non-PAO biomass (OHO) under anoxic conditions, which includes (i) reduction of NO_3 to NO_2; (ii) reduction of NO_2 to NO; (iii) reduction of NO to N_2O; (iv) reduction of N_2O to nitrogen gas

(N_2). The incomplete reduction of NO_2 into N_2 may lead to the accumulation of N_2O, which is also included in the model.

The physical sub-model is characterized by 6 parameters and 2 state variables. The physical sub-model allows to assess the contribution of the membrane module in the organic matter removal by means of the cake layer formed onto the membrane and the physical separation throughout the membrane (Mannina et al., 2018a).

Biological and physical sub-models are interlinked by means of the total suspended solids (TSS) and SMP concentration inside the MBR. The model also evaluates the total GHG emissions (both in terms of N_2O and CO_2) as the sum of direct and indirect emissions of both sub-models. Further details regarding the model can be found in the literature (Mannina et al., 2018a-b).

2.2 Pilot plant description

A University of Cape Town (UCT) MBR pilot plant (composed by anaerobic, anoxic and aerobic reactors in series) has been taken as case study (Mannina et al., 2016). The influent wastewater (a mixing between real and synthetic wastewater) flow rate was equal to 20 L h^{-1} with constant carbon-nitrogen ratio features (equal to 10 mgCODmgTN^{-1}) (Mannina et al., 2018a). The solid/liquid separation occurred by means of an ultrafiltration hollow fiber membrane (PURON® - pore size of 0.03 μm and membrane surface of 1.4 m^2) located inside the MBR bioreactor (permeate flux of 21 Lm^2h^{-1}). For a more detailed description of the pilot plant and sampling campaign, the reader is referred to Mannina et al. (2016).

2.3 Scenario analysis

Three scenarios have been considered in this study: i. Scenario 0 – Benchmark with an open-loop air flow control inside the aerobic reactor; ii. Scenario 1 – where a closed-loop cascade ammonia proportional-integral (PI) control is applied inside the aerobic reactor to establish the DO setpoint and consequently the air flow rate; iii. Scenario 2 – where a closed-loop cascade PI control based on ammonia and nitrite concentration inside the aerobic reactor is applied to establish the DO setpoint and consequently the air flow rate. Scenario 2 aims at reducing the amount of N_2O emission from the aerobic reactor. The scenario analysis has been employed by using the mathematical model described above and considering 42 simulation days.

2.3.1 Aeration control strategies – scenarios 1 and 2

Figure 1 shows the closed-loop aeration control strategies applied for scenarios 1 and 2.

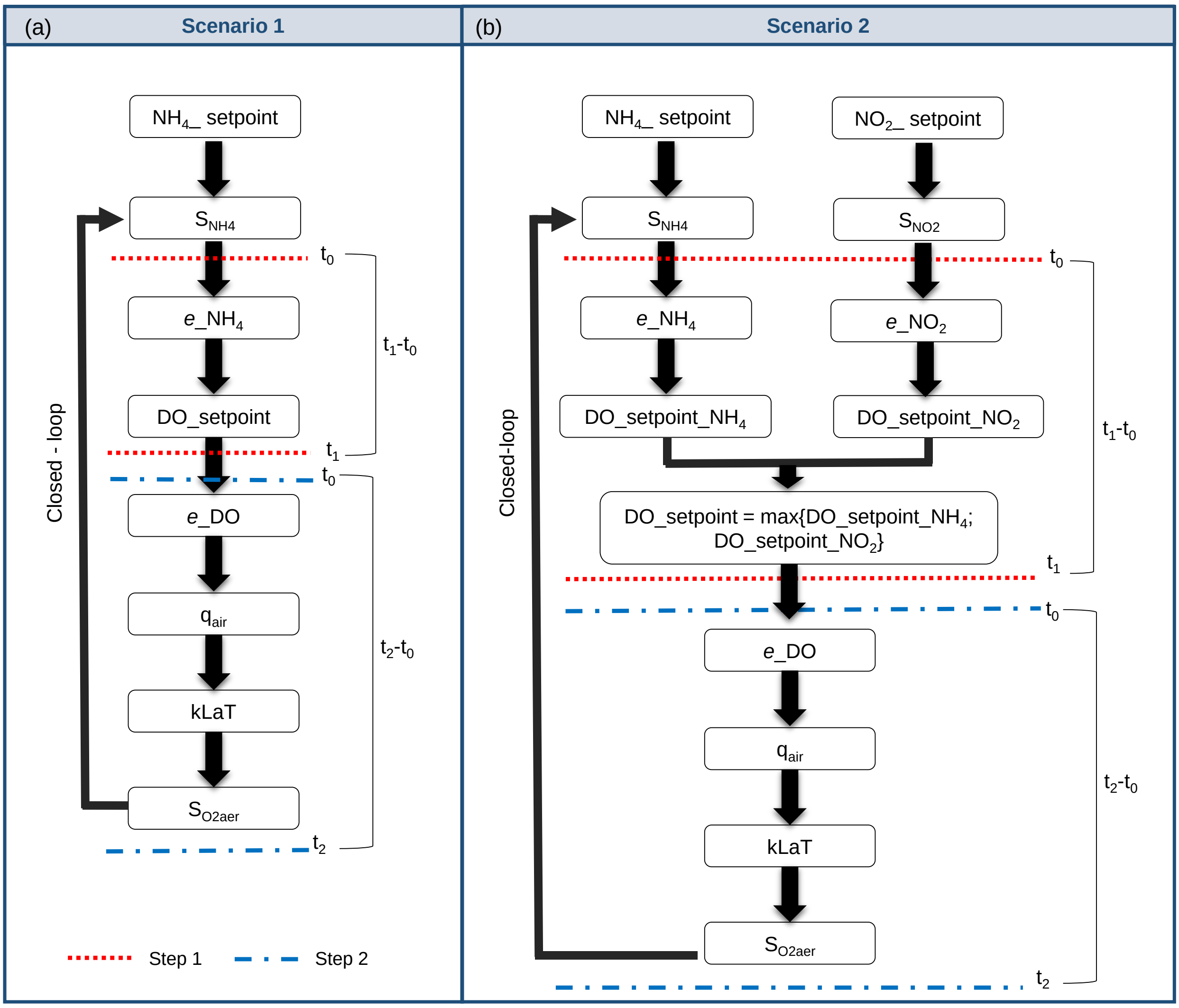

Figure 1. Schematic representation of two-step cascade control adopted for Scenario 1 (a) and Scenario 2 (b). NH_4_setpoint = set point of ammonia concentration inside the aerobic reactor; NO_2_setpoint = set point of nitrite concentration inside the aerobic reactor; S_{NH4}, S_{NO2} and S_{O2aer} = ammonia, nitrite and dissolved oxygen concentration inside the aerobic reactor, respectively; DO_setpoint = set point of the dissolved oxygen concentration inside the aerobic reactor; DO_setpoint_NH_4 = set point of the dissolved oxygen concentration inside the aerobic reactor established on the basis of ammonia control (S_{NH4}); DO_setpoint_NO_2 = set point of the dissolved oxygen concentration inside the aerobic reactor established on the basis of nitrite control (S_{NO2}); e_DO, e_NH_4 and e_NO_2 error of the dissolved oxygen, ammonia and

nitrite concentration; q_{air} = air flow rate inside the aerobic reactor; kLaT = oxygen transfer coefficient; t_0, t_1 and t_2 = time related to the control interval during Step 1 (t_0 and t_1) and Step 2 (t_0 and t_2).

For Scenario 1, a similar approach to previous literature was employed (Sun et al., 2016). In particular, an aeration control strategy algorithm was implemented as a two-step feedback control based on the NH_4 and DO concentration (first step), and air flow (second step) (Figure 1a).

The first action in the aeration control strategy is to establish the ammonia set point (NH_4_setpoint) inside the aerobic reactor (Figure 1a). Then, the ammonia error (e_NH_4, as mg.L^{-1}) is calculated as the difference between NH_4_setpoint and the NH_4 concentration within the aerobic reactor (S_{NH4}, as mg.L^{-1}) (Equation 1).

$$e\_NH_4 = NH_4\_setpoint - S_{NH4} \quad (1)$$

The NH_4_setpoint is manually assigned on the basis of the effluent requirements. If the concentration of NH_4 in the aerobic tank is higher than NH_4_setpoint ($e\_NH_4 < 0$), the aeration system insufflates more air in order to increase the nitrification and reduce the ammonia concentration in the bioreactor. Conversely, if $e\_NH_4 > 0$, the air flow rate is reduced to ensure that the ammonia concentration in the tank reaches a stable value with respect to the NH_4_setpoint.

The value of e_NH_4 is applied to calculate the DO setpoint (DO_setpoint), which represents the DO concentration of interest that may lead to a NH_4 stable value (Equation 2) (Figure 1a).

$$DO_{\_setpoint} = Bias_1 + K_{p1} \cdot \ e\_NH_4 + K_{p1} \cdot \frac{1}{\tau_1} \cdot \int_{t_{1-t_0}}^{t_0} e\_NH_4 \cdot dt \quad (2)$$

where $Bias_1$, K_{p1} and τ_1 are control parameters (Sun et al., 2016), t_0 represents the initial time of the control (and its equal to zero), t_1-t_0 is the control interval (assumed equal to 30 minutes in this simulation) and *e_NH4·dt* is the derivate of the NH_4 error during the control interval. Other acronyms were previously described. In Equation 2 the term $Bias_1$ represents the baseline NH_4 error, while the term $K_{p1} \cdot \ e\_NH_4$ is the NH_4 real-time error and the term $K_{p1} \cdot \frac{1}{\tau_1} \cdot \int_{t_{1-t_0}}^{t_0} e\_NH_4 \cdot dt$ represents the NH_4 error accumulated during the control interval.

Therefore, in the first step, the ammonia-based and DO-based control strategies are combined before applying the cascade control in the second step. At the beginning of the second step, the calculated DO_setpoint is used to obtain the DO error (e_DO, as mg.L^{-1}) related to the DO concentration (S_{O2aer}, as mg.L^{-1}) inside the aerobic reactor, calculated as shown in Equation 3 (Figure 1a).

$$e\_DO = DO\_setpoint - S_{O2aer} \quad (3)$$

The error related to the DO concentration is used to obtain the air flow rate that has to be supplied by the aeration system (Equation 4). If e_DO < 0, the aeration system reduces the q_{air} value and vice versa.

$$q_{air} = Bias_2 + K_{p2} \cdot\ e\_DO + K_{p2} \cdot \frac{1}{\tau_2} \cdot \int_{t_{3-t_2}}^{t_2} e\_DO \cdot dt \quad (4)$$

where $Bias_2$, K_{p2} and τ_2 are controller parameters (Sun et al., 2016), t_2-t_0 is the control interval (assumed as the 30 minutes that succeed the previous step) and *e_DO·dt* is the derivate of the DO error during the control interval.

The value of q_{air} is used by the model to obtain the oxygen transfer coefficient (kLaT), which is introduced in the oxygen (namely, S_{O2aer}) mass-balance equation according to the ASM approach (Henze et al., 2000). The term kLaT is calculated according to Equation 5.

$$kLaT = k_1 * (1 - \exp^{(k_2 \cdot q_{air})}) \quad (5)$$

where k_1 and k_2 are parameters related to the MBR plant. Table 1 contains the values of the control parameters mentioned in this section.

The control strategy related to Scenario 2 is an extension of Scenario 1. The first phase of control strategy applied to Scenario 2 includes a cascade PI nitrite controller in the aerobic reactor to calculate the DO setpoint (Figure 1b). More specifically, during the first step, two DO setpoints are calculated: 1) DO_setpoint_NH_4, evaluated based on the ammonia control analogously to Scenario 1; 2) DO_setpoint_NO_2 evaluated on the basis of the nitrite control.

DO_setpoint_NO_2 is evaluated according to Equation 6.

$$DO_{\_setpoint\_NO2} = Bias_{1,NO2} + K_{p1;NO2} \cdot\ e\_NO_2 + K_{p1,NO2} \cdot \frac{1}{\tau_{1,NO2}} \cdot \int_{t_{1-t_0}}^{t_0} e\_NO_2 \cdot dt \ [6]$$

where $Bias_{1,NO2}$, $K_{p1,NO2}$ and $\tau_{1,NO2}$ are controller parameters related to nitrite control and e_NO_2 is the NO_2 error during the control interval. e_NO_2 represents the difference between the nitrite set point (NO_2_setpoint) and the actual NO_2 concentration (S_{NO2}) inside the aerobic reactor.

The maximum value between DO_setpoint_NO_2 and DO_setpoint_NH_4 is then selected to evaluate the DO error (e_DO) during the second control step (Figure 2b).

The second control step of Scenario 2 is identical to Scenario 1.

Table 1. Summary of the parameters of the control algorithm applied to Scenario 1 and Scenario 2

Control Parameter	Value	Unit	Reference
NH_4_setpoint	10	$mg.L^{-1}$	(this study)
$Bias_1$	1	$mg.L^{-1}$	Sun et al. (2016)
K_{p1}	-1	$mgDO.L^{-1}/ mgN.L^{-1}$	Sun et al. (2016)
τ_1	20	minutes	Sun et al. (2016)
NO_2_setpoint	0.5	$mg.L^{-1}$	(Solis et al., 2019)
$Bias_{1,NO2}$	1	$mg.L^{-1}$	Sun et al. (2016)
$K_{p1,NO2}$	-1	$mgDO.L^{-1}/ mgN.L^{-1}$	Sun et al. (2016)
$\tau_{1,NO2}$	30	minutes	Sun et al. (2016)
$Bias_2$	600	$m^3.d^{-1}$	Sun et al. (2016)
K_{p2}	500	$m^3air.d^{-1}.h^{-1}$	Sun et al. (2016)
τ_2	15	minutes	Sun et al. (2016)
k_1	200	-	Mannina et al. (2018a)
k_2	-0.25	-	Mannina et al. (2018a)

The control of DO is enhanced by the two-step cascade control leading to to an improvement of the nitrification process by acting on the NH_4 oxidation.

2.4 Performance indicators

The influence of the open and closed-loop dynamic aeration controls is assessed by the following Performance Indicators (PIs): Effluent Quality Index (EQI, kg Pollutant m^{-3}) for both liquid (EQI_{LIQ}) and gas (EQI_{GAS}) flows; oxygen-to-total-Kjeldahl-nitrogen ratio (RON, gO_2 gNH_4^{-1}); ratio nitrate-ammonia (R_{NAT}, gNO_3 gNH_4^{-1}); Operating Costs (OC, as euro m^{-3}); Effluent Fine (EF, euro m^{-3}); CO_2 and N_2O emissions ($kgCO_{2,eq}$ m^{-3}); direct (DE, $kgCO_{2,eq}$ m^{-3}) and indirect (IE, $kgCO_{2,eq}$ m^{-3}) GHG emissions.

The EQI quantifies the pollution load discharged into the water body (kg pollution units/day or kg pollution units/treated volume) Equation 7) (Nopens et al., 2010; Mannina et al., 2019).

$$EQI_{LIQ} = \frac{1}{T*1000}\int_{t0}^{t1}[\sum P_k\,(\mathrm{t})] \cdot Q_{eff}\, dt \quad (7)$$

where t_0 indicates the initial time, t_1 the end of the simulation period, *Qeff* is the accumulated effluent flow, *dt* is the simulation period, 1000 is the conversion factor from g m^{-3} to kg m^{-3}, P_k in the pollutant load of each component in a time *t*, which is expressed according to Equation 8.

$$P_k = \beta_x \cdot C_k \quad (8)$$

where β_x is the weighting factor of every single pollutant and C_k is the pollutant's concentration (mg·L^{-1}). The following components (*k*) were considered in this study: chemical oxygen demand (COD_e), ammonia (S_{NH4e}), nitrate (S_{NO3e}), nitrous oxide (S_{N2Oe}) and phosphate (S_{POe}), for which the following weighting factors were used (Mannina & Cosenza, 2015): β_{COD}=1, β_{NH}=20, β_{NO3}=20, β_{N2O}=50 and β_{PO}=50.

The EQI_{GAS} was also adopted by Mannina et al. (2019) considering the gas flow rate (Q_{offgas}) and the off-gas concentration in terms of CO_2 and N_2O ($Offgas_{,CO2}$ and $Offgas_{,N2O}$, respectively). The adopted β_i values for EQI_{GAS}, defined for each GHG are β_{N2O}=50 and β_{CO2}=50.

RON provides a relationship between the oxygen supplied to the plant and the Total Kjeldahl Nitrogen (TKN) in the influent (Boiocchi et al., 2017a). Considering the main purpose of this work, RON is a key indicator to verify the plant's performance since it allows understanding how much of the oxygen provided to the system was used to oxidize the influent ammonium. RON is calculated according to Equation 9.

$$R_{ON} = \frac{\sum_{i=1}^{n} k_L a_{AER,i} \cdot V_{AER,i} \cdot (SO_{2,SAT,AER,i} - SO_{2,AER,i})}{Q_{in} \cdot S_{NH,in}} \quad (9)$$

where $k_{LaAER,i}$ is the oxygen mass transfer coefficient of the aerated tank i; $V_{AER,i}$ is the volume of the i-th aerobic tank; $S_{O2,SAT,i}$ is the oxygen saturation concentration of i-th aerobic tank; $S_{O2,AER,i}$ is the oxygen concentration in the aerobic tank i; Q_{in} is the inlet flow rate fed to the biological zone; and $S_{NH,in}$ is the inlet ammonium nitrogen fed to the biological zone.

R_{NAT} is a performance indicator representing the ratio between the nitrate produced and the ammonia oxidized in the aerobic reactor (Boiocchi et al., 2017b). The results of R_{NAT} can be used as a reference to understand the emissions of N_2O; indeed, R_{NAT} indicates the degree of nitrification within the aerobic zone and the relation between the autotrophic biomass. For instance, R_{NAT} = 1 gNO_3 gNH_4^{-1} means that all NO_2 produced by the AOB is converted into NO_3 by the NOB. R_{NAT} is calculated according to equation 10:

$$R_{NAT} = \frac{NO^-_{3,OUT,AER} - NO^-_{3,IN,AER}}{NH^+_{4,IN,AER} - NO^+_{4,OUT,AER}} \quad (10)$$

where $S_{NO3,IN,AER}$ and $S_{NO3,OUT,AER}$ represent, the nitrate influent and effluent concentration inside the aerobic reactor, respectively; $S_{NH4,IN,AER}$ and $S_{NH4,OUT,AER}$ are the NH_4 concentrations of the influent and effluent of the aerobic reactor, respectively.

The operational costs - OC (€/treated volume) represents the sum of three costs (Vanrolleghem and Gillot, 2002; Guerrero et al., 2011): the costs related to the chemical consumption for membrane cleaning (CC, as €/ treated volume), the energy demand (*e*D, €/ treated volume) and effluent fine (EF) related to pollutants discharged (in accordance with Italian regulations), according to Equation 11:

$$OC = eD \cdot \gamma_e + CC + EF \quad (11)$$

where γ_e represents the cost per kWh. Italian rates are 0.21 € / kWh.

The membrane cleaning cost CC is calculated considering a typical membrane cleaning protocol (i.e., including a chemical solution composed of 500 ppm of NaOCl and 2,000 ppm of citric acid, with a cost of 0.48€ per chemical cleaning), which was held only when the transmembrane pressure (TMP) reached a value higher than 60kPa as suggested by the membrane manufacturer. The EF was assessed in accordance with Mannina & Cosenza (2015).

The energy demand *e*D (kWh) is calculated according to Equation 12:

$$eD = P_w + P_{eff} + P_s + P_m \quad (12)$$

where P_w, P_{eff}, P_s, and P_m represent, respectively, the energy consumption for the air blowers, permeate extraction, recycle pumps and mixers; P_w, P_{eff}, and P_s are calculated according to Mannina et al. (2019). P_{eff} is proportional to the transmembrane pressure (TMP) to be imposed to the membrane to obtain a constant permate flow rate Mannina et al. (2019). P_w was calculated for both aerobic (P_{w3}) and membrane bioreactor (P_{w4}), while P_m comprised the energy used for constantly mixing the anaerobic and anoxic tanks. It was assumed that both tanks required 0.008 kWh per m^3 tank volume (Tchobanoglous et al., 2003; Maere et al., 2011).

Total direct emissions (DE) represent the sum between CO_2 and N_2O stripped from the liquid to the gas phase (Mannina et al., 2018a), while the indirect emissions (IE) can be evaluated by multiplying *e*D by $\gamma_{CO,}$ (equal to 0.245 $kgCO_{2eq}$ /kWh); γ_{CO} represents the specific CO_2 emission due to the energy consumption (EIA, 2009). DE and IE are both expressed in terms of carbon equivalent ($kgCO_{2,eq}$ m^{-3}) with the aim to obtain comparable units in terms of GHG emissions. For a more detailed description of the performance indicators, the reader is referred to Mannina et al. (2019).

3. Results and discussion

3.1 Scenario 0

Figure 2a reports the patterns of the air flow rate supplied to the aerobic reactor, along with the influent ammonia concentration ($S_{NH4,IN}$) and of the dissolved oxygen concentration inside the aerobic reactor (S_{O2aer}) for Scenario 0. Figure 2b shows the trend of the total power consumption (of the entire plant) inside the pilot plant for Scenario 0.

Data reported in Figure 2a show that, during Scenario 0 no air flow control has been implemented. Indeed, a constant air flow rate (21.6 m^3d^{-1}) was supplied to the aerobic reactor disregarding the amount of influent ammonia to be oxidized and the amount of dissolved oxygen inside the aerobic reactor.

As shown in Figure 2a, the influent ammonia concentration has considerable fluctuation during the 42 days of simulation. Indeed, ammonia ranged between 19 and 67 mg L^{-1}. Despite the ammonia variability, the high air flow rate supplied to the aerobic reactor led to a quite high DO concentration inside the aerobic reactor.

Indeed, the average S_{O2aer} maintained inside the aerobic reactor was equal to 7.2 mg L^{-1}. This latter value is much higher than the dissolved oxygen value suggested in literature for the aerobic processes (i.e., 1.5-2 mg L^{-1}) (Metcalf, & Eddy, 2003). Consequently, an high energy consumption has been observed throughout the entire simulation period. On average, 4.8 kWh m^{-3} of energy was consumed by the plant. This latter value is almost doubles the average power consumption reported for MBRs treating similar wastewater (Krzeminski et al., 2012). Almost 87% of the total power consumption was related to the aeration inside the aerobic reactor. This result suggests that the open-loop aeration scenario is highly inefficient and the high energy consumption can be translated into potential energy recovery for the plant under study (Solon et al., 2017).

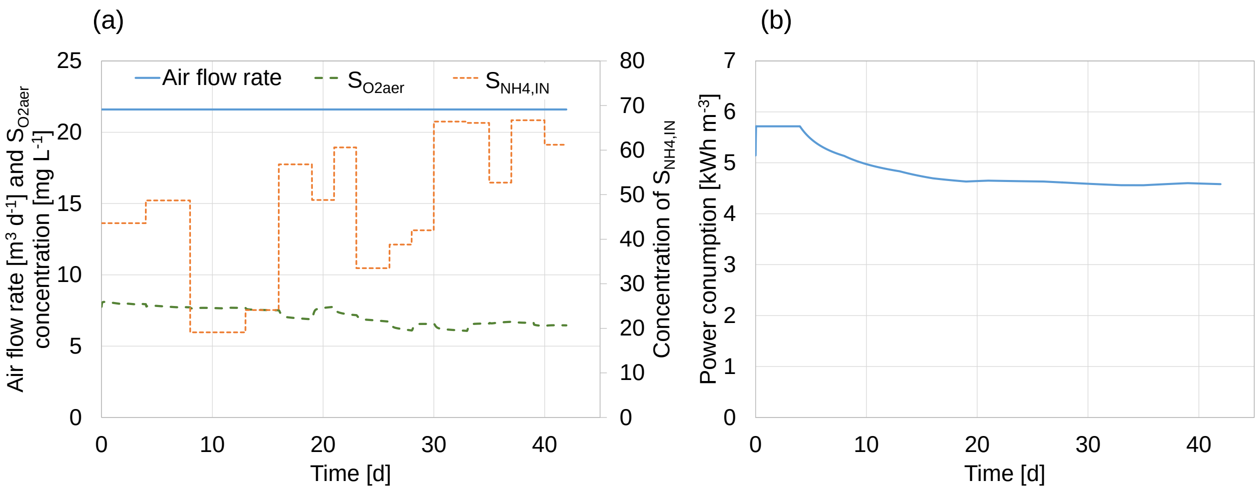

Figure 2. The pattern of airflow rate and dissolved oxygen (S_{O2ae}) within the aerobic reactor and influent ammonia concentration ($S_{NH4,IN}$) (a) and power consumption (b) for Scenario 0.

3.2 Scenario 1

In Figure 3a, the trends of q_{air}, S_{O2aer} in the aerobic reactor and $S_{NH4,IN}$ for Scenario 1 are reported. Figure 3b shows the total power consumption inside the pilot plant for Scenario 1 over the modelling period.

As shown in Figure 3a the air flow rate during scenario 1 varies according to $S_{NH4,IN}$ since the DO setpoint is controlled on the basis of the ammonia inside the aerobic reactor. Thus, results show a reduction in air flow rate and DO inside the aerobic reactor. In particular, the average air flow supplied to the aerobic reactor is equal to 11.5 m^3d^{-1} (almost half of the value reported in Scenario 0). While the dissolved oxygen concentration inside the aerobic reactor ranges between 0.7 and 7.2 mg L^{-1}. It is important to highlight the beneficial effect of controlling air flow rate in terms of power consumption. Indeed, the average power consumption was equal to 3.3 kWh m^{-3}, which is lower than that obtained for Scenario 0. Thus, a substantial reduction (namely, 32%) in terms of power consumption occurred during Scenario 1 with respect to Scenario 0. This value is slightly higher than that obtained by Sun et al. (2016) (from 15 to 20%) for a full-scale MBR where the same control strategy of Scenario 2 was applied. The difference between both studies may be related to the fact that Sun et al. (2016) presented results considering the whole WWTP, while the current work is focused only on the activated sludge process and MBR.

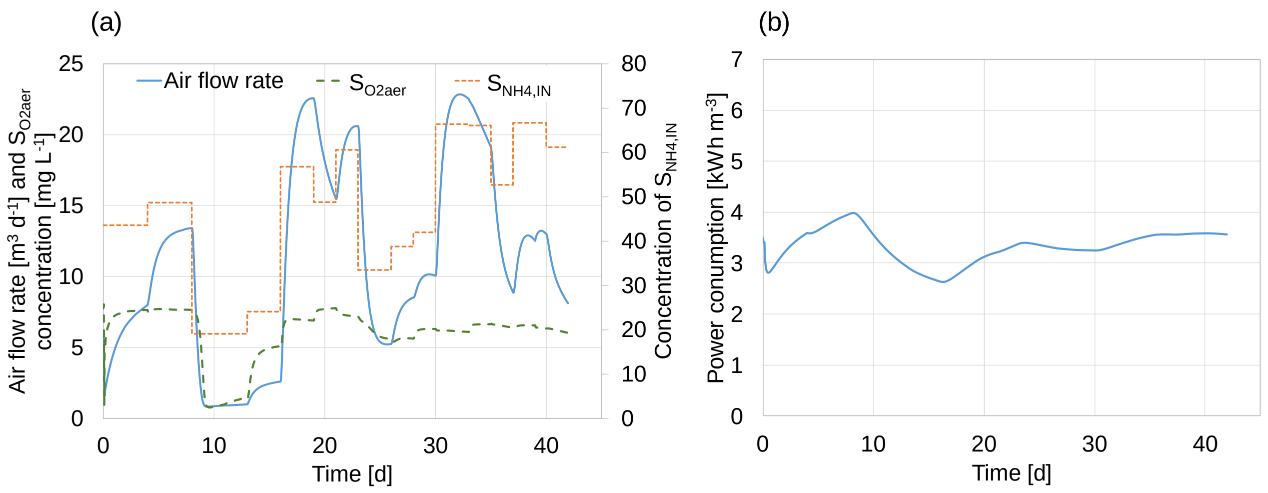

Figure 3. The pattern of air flow rate supplied to the aerobic reactors and dissolved oxygen inside the aerobic reactor, and influent ammonia concentration (a) and power consumption (b) for Scenario 1.

3.3 Scenario 2

Figure 4a shows the trend of the air flow rate and S_{O2aer} in the aerobic reactor and of $S_{NH4,IN}$ for Scenario 2. Figure 4b shows the total power consumption inside the pilot plant for Scenario 2 throughout the modelling period.

Results reported in Figure 4a show a substantial reduction, respect to previous scenarios, both in terms of air flow rate and S_{O2ae}. Indeed, differently to previous scenarios, the aeration flow rate was adjusted not only with respect to the ammonia inside the aerobic reactor, but also taking into account the nitrite concentration. The air flow rate, and consequently S_{O2aer}, follows the trend of influent ammonia. In particular, the air flow rate varied between 0.76 and 21.6 $m^3 d^{-1}$. which are lower respect to previous scenarios. The obtained value of oxygen concentration (S_{O2aer}) is able to ensure proper aerobic conditions inside the aerobic reactor, with values ranging between 0.45 and 7.2 mg L^{-1}. The substantial decrease of the average air flow rate provided a very low power consumption in the plant under study (equal to 0.7 kWh m^{-3}). The obtained power consumption is in accordance with previous studies related to real MBR plants, which found an energy-specific consumption ranging between 0.62 and 0.75 kWh m^{-3} (Giesen et al., 2008; Wallis-Lage and Levesque, 2009; Fenu et al., 2010). As discussed above, these results have substantial implications in terms of indirect and direct GHG emissions.

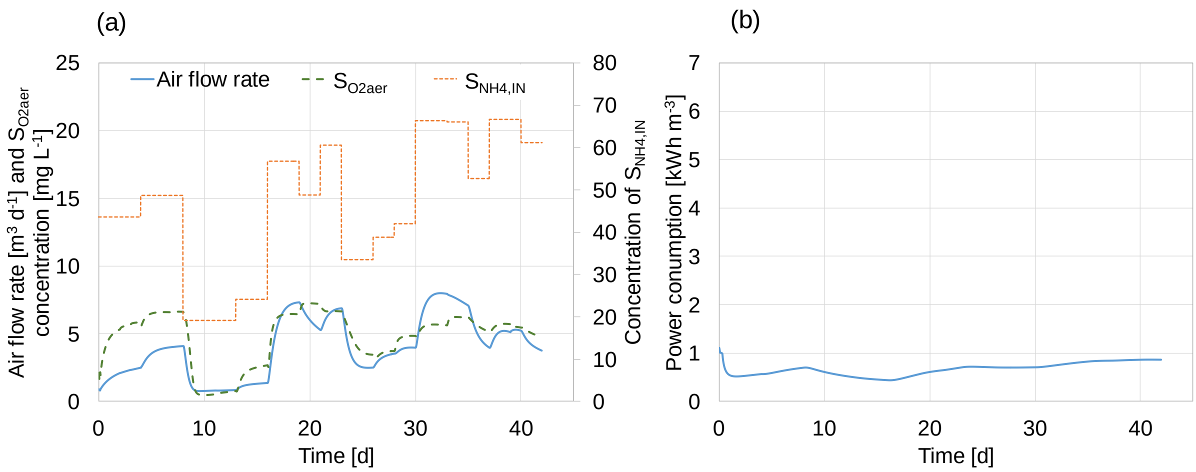

Figure 4. The pattern of airflow rate inserted inside the aerobic reactors, dissolved oxygen inside the aerobic reactor – S_{O2aer} and influent concentration of ammonia - $S_{NH4,IN}$ (a) and power consumption (b) for Scenario 2.

3.4 Comparison among scenarios

In this section, the comparison of the three analyzed scenarios is presented in terms of PIs. More in detail, Figure 5 reports the results in terms of average effluent fine (EF), operating costs (OC), R_{NAT}, RON, direct and indirect emissions, and dissolved N_2O inside the aerobic reactor (S_{N2Oaer}) for each analyzed scenario. For sake of completeness, in Table 2 the values of all PIs obtained for each scenario are also reported.

As shown in Figure 5a, the EF value was not affected by the control strategies, ranging between 0.099 and 0.108 € m^{-3} (Table 2). This slight difference is due to twofold reasons: i. the membrane presence, ii. the sufficient dissolved oxygen for all scenarios in aerobic reactor. Indeed, for all scenarios, an excellent effluent quality has been achieved due to the membrane solid/liquid separation, which guarantees the retaining of all suspended compounds. Moreover, the dissolved compounds have been adequately removed thanks to the sufficient dissolved oxygen concentration within the aerobic reactor during the all scenarios. Therefore, the air flow rate reduction did not affect the biological treatment because even the minimal DO concentration during the simulations was enough for biomass survival and sufficient for the system adequate performance in terms of nutrient removal.

On the other hand, the reduction of the air flow rate had substantial implications in terms of operating costs. As reported in Figure 5a, the obtained average value of operating costs was equal to 1.16, 0.78 and 0.41 € m^{-3} for Scenarios 0, 1 and 2, respectively, presenting a reduction of 35% of operating costs ranging from Scenario 0 to Scenario 1 and of 64% from Scenario 0 to Scenario 2. This latter result is in accordance with previous studies stating that aeration has a key role in the operating costs (Xiao et al., 2014; Sun et al., 2016) and confirm the great advantage in aeration-based control strategies. Despite the energy demand due to the membrane aeration (P_{w4}) was not controlled/varied by means of the controller, the amount of energy required for the permeate extraction (P_{eff}) was influeced by the aeration of the aerabic reactor. Indeed, from scenario 0 to scenario 2, it was obtained a TMP reduction of 30%.

Both R_{NAT} and RON have been reduced during the closed-loop scenarios with respect to Scenario 0. Indeed, as reported in Figure 5b the obtained average value of R_{NAT} was equal to 0.36, 0.34 and 0.22 gNO_3 gNH_4^{-1} for Scenarios 0, 1 and 2, respectively. The decrease of R_{NAT} is mainly due to the low dissolved oxygen concentration inside the aerobic reactor. However, the R_{NAT} value is always quite high to guarantee the low nitrite accumulation inside the system (Boiocchi et al., 2016). In terms of RON a reduction from 6 to 5.4 gO_2 gNH_4^{-1} was obtained from Scenario 0 to Scenario 2 (Figure 5c). The RON value obtained for Scenario 2 is in accordance with literature (Boiocchi et al., 2017a). Indeed, Boiocchi et al. (2017a) reported that RON equal or higher than 5.2 gO_2 $gTKN^{-1}$ represents the optimal value for obtaining the best trade-off between the ammonia conversion rate and the N_2O emission (i.e., the lowest N_2O emission at the highest ammonium oxidation). With this regard, Figure 5d reports a reduction of direct GHG emission for Scenario 2 in comparison to the other two scenarios. In particular, the direct GHG emission reduced from 0.52 to 0.47 $kgCO_{2eq}$ m^{-3} (from Scenario 0 to Scenario 2). This reduction is mainly due to the aforementioned N_2O

emissions. The trend of S_{N2Oaer} for all scenarios is reported in Figure 5e and shows a lower concentration for Scenario 2. This result is due to two aspects: i. the improvement of biological processes in Scenario 2 thanks to the adequate air flow rate; ii. the reduction of the air flow rate in Scenario 2 led to the reduction of the N_2O stripped from the soluble form to the off-gas.

In terms of indirect emission, a substantial reduction (namely, 81%) occurred from Scenario 0 to Scenario 2 (from 1.12 $kgCO_{2eq}$ m^{-3} for Scenario 0 to 0.21 $kgCO_{2eq}$ m^{-3} for Scenario 2). This reduction is mainly due to the lower air flow rate supplied in Scenario 2.

The results obtained in this study are important to encourage the scattering of the MBR technology because demonstrate that the optimization of the membrane systems in terms of their declared major issues (i.e., energy consumption and operating costs) may be achieved by simplified automatic systems. However, further studies are recommended to assess the effect of automatic controls and aeration-based control systems over membrane fouling issues.

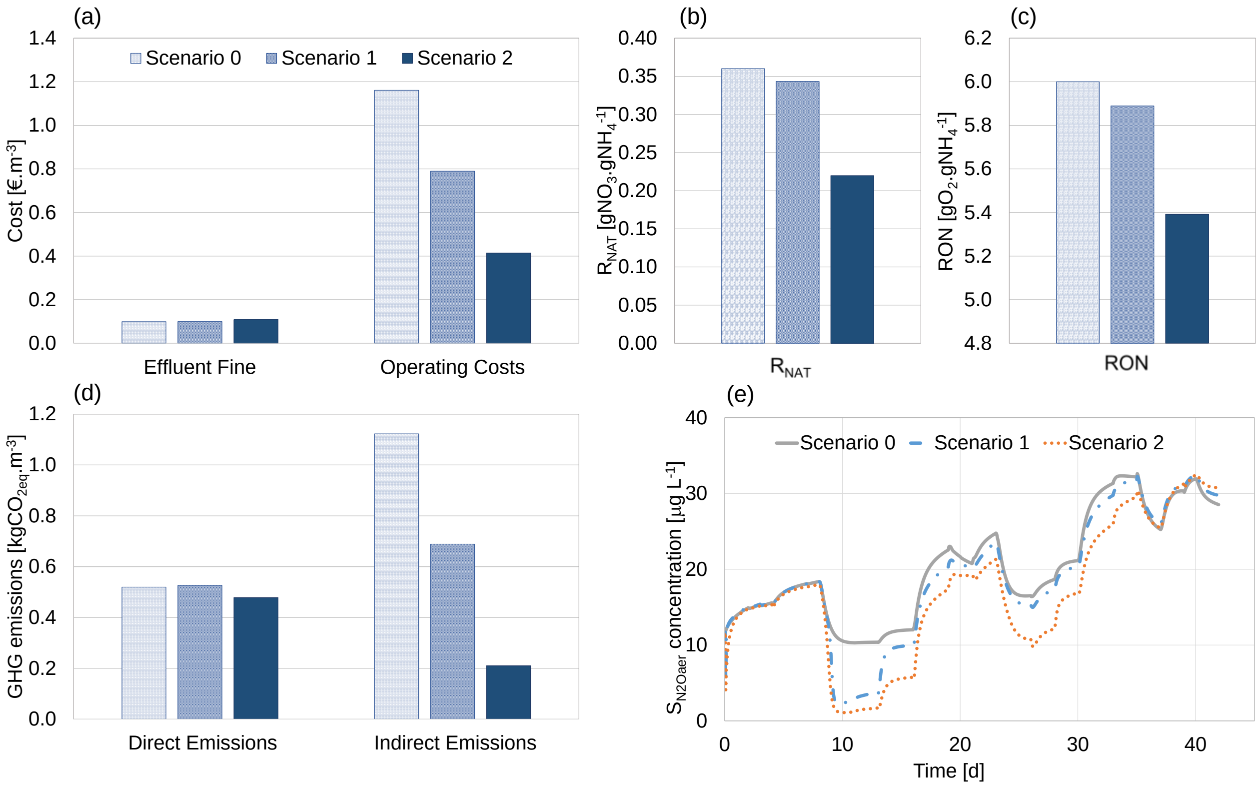

Figure 5. Average effluent fine (EF) and operating costs (OC) (a), average value of R_{NAT} (b), average value of RON (c), direct and indirect emissions (d), pattern of dissolved N_2O inside the aerobic reactor – S_{N2Oaer} for each analyzed scenario.

Table 2. Summary of the values of PIs obtained for Scenarios 0, 1 and 2)

PIs →	**R_{NAT}**	**RON**	**$EQI_{LIQ,TOT}$**	**$EQI_{GAS,TOT}$**	**Effluent Fine**	**Operating Costs**	**Energy Consumption**	**Indirect Emissions**	**Direct Emissions**
Unit→	[gNO_3 gNH_4^{-1}]	[gO_2 gNH_4^{-1}]	[kg m^{-3}]	[kg m^{-3}]	[€ m^{-3}]	[€ m^{-3}]	[kWh m^{-3}]	[$kgCO_{2,eq}$ m^{-3}]	[$kgCO_{2,eq}$ m^{-3}]
Scen. 0	0.360	6.0	15.49	55.39	0.099	1.16	4.8	1.12	0.52
Scen. 1	0.343	5.9	15.55	55.47	0.099	0.79	2.8	0.69	0.53
Scen. 2	0.220	5.4	16.65	55.65	0.108	0.41	0.8	0.21	0.48

4. Conclusions

The key findings of the study suggest that it is possible to find a trade-off between effluent quality, GHG emissions, energy consumption and operating costs by applying a closed-loop control system. These findings were achieved by simultaneously controlling ammonia and nitrite concentrations within the aerobic reactor. These results have substantial importance while disseminating the application of aeration-based controls in the MBR field, since the optimization of the MBR major issues may be achieved by the use of simplified automatic systems. Future studies could be performed in order of testing the PI control strategy developed here with other MBR plants configuration.

REFERENCES

1. Benyahia, B., Sari, T. Cherki, B., Harmand, J., 2013. Anaerobic membrane bioreactor modeling in the presence of Soluble Microbial Products (SMP) – the Anaerobic Model AM2b. Chemical Engineering Journal 228 (2013) 1011–1022.
2. Boiocchi, R., Gernaey, K. V., & Sin, G. (2016). Control of wastewater N_2O emissions by balancing the microbial communities using a fuzzy-logic approach. IFAC-PapersOnLine 49-

7, 1157–1162.

3. Boiocchi, R., Gernaey, K. V., & Sin, G. (2017a). A novel fuzzy-logic control strategy minimizing N_2O emissions. Water Research, 123, 479–494.
4. Boiocchi, R., Gernaey, K. V., Sin, G. (2017b). Understanding N_2O formation mechanisms through sensitivity analyses using a plant-wide benchmark simulation model. Chemical Journal Engineering 317, 935–951.
5. Bozkurt, H., van Loosdrecht, C. M., Gernaey, V., Sin, G. (2016). Optimal WWTP process selection for treatment of domestic wastewater – A realistic full-scale retrofitting study. Chemical Engineering Journal 286, 447-458.
6. Dalmau, M., Monclús, H., Gabarrón, S., Rodriguez-Roda, I., Comas, J. (2014). Towards integrated operation of membrane bioreactors: Effects of aeration on biological and filtration performance. Bioresour. Technol. 171, 103-112.
7. Domingo-Félez, C. and Smets, B.F., 2020. Modelling N_2O dynamics of activated sludge biomass: Uncertainty analysis and pathway contributions. Chemical Engineering Journal 379, 122311.
8. EIA - United States Energy Information administration, 2009. Annual Energy Outlook 2009 - with Projections to 2030 DOE/EIA-0383(2009), Washington, DC.
9. Fenu, A., Roels, J., Wambecq, T., De Gussem, K., Thoeye, C., De Gueldre, G., Van De Steene, B. (2010) Energy audit of a full scale MBR system. Desalination 262 (1–3), 121–128.
10. Ferrero, G., Monclús, H., Buttiglieri, G., Comas, J., Rodriguez-Roda, I. (2011). Automatic control system for energy optimization in membrane bioreactors. Desalination 286 (1 – 3), 276 – 280. hfm
11. Ferrero, G., Rodriguez-Roda, I. Comas, J., (2012). Automatic control systems for submerged membrane bioreactors: A state-of-the-art review. Water Research 46, 3421-3433.
12. Flores-Alsina, X., Corominas, L., Snip, L.,Vanrolleghem, P. A. (2011). Including

greenhouse gas emissions during benchmarking of wastewater treatment plant control strategies. Water Research 45, 4700 – 4710.

13. Gabarrón, S., Dalmau, M., Porro, J., Rodriguez-Roda, I., Comas, J. (2015). Optimization of full-scale membrane bioreactors for wastewater treatment through a model-based approach. Chemical Engineering Journal 267, 34 – 42.
14. Giesen, A., Van Bentem, A., Gademan, G. & Erwee, H., (2010). Lessons learnt in facility design, tendering and operation of MBR's for industrial and municipal wastewater treatment. In: Proceedings of WISA Biennial Conference and Exhibition, paper 102, Sun City, South Africa
15. González, E., Luis, O. D., Rodríguez-Gómez, V. L. E., Rodríguez-Sevilla, J., (2018). Feedback control system for filtration optimisation based on a simple fouling model dynamically applied to membrane bioreactors. Journal of Membrane Science 552, 243 – 252.
16. Guerrero, J., Guisasola, A., Vilanova, R., Baez, J. A. (2011). Improving the performance of a WWTP control system by model-based setpoint optimization. Environmental Modelling & Software 26, 492-497.
17. Guo, W., Ngo, H., Li, J. (2012). A mini-review on membrane fouling. Bioresource Technology 122, 27 – 34.
18. Henze, M., Gujer, W., Mino, T., van Loosdrecht, M.C.M., 2000. Activated Sludge Models ASM1, ASM2, ASM2d, and ASM3. IWA Scientific and Technical Report n. 9. IWA Publishing, London, UK.
19. Hiatt, W. C., Grady Jr, C.P.L. (2008). An updated process model for carbon oxidation, nitrification, and denitrification. Water Environ. Res. 80, 2145–2156.
20. Kalboussi, N., Harmand, J. Rapaport, A., Bayene, T., Ellouze, F., Amar, N.B., (2018). Optimal control of physical backwash strategy - towards the enhancement of membrane filtration process performance. Journal of Membrane Science 545, 38–48

21. Krzeminski, P., Leverette, L., Malamis, S., Katsou, E., (2017). Membrane bioreactors – A review on recent developments in energy reduction, fouling control, novel configurations, LCA and market prospects. Journal of Membrane Science 527, 207–227.
22. Krzeminski, P., Jaap van der Graaf, H.J.M. van Lier, J.B., 2012. Specific energy consumption of membrane bioreactor (MBR) for sewage treatment. 2 Water Science & Technology 65(2), 380-392.
23. Koutsou, O.P., Gatidou, G., Stasinakis A. S. (2018). Domestic wastewater management in Greece: greenhouse gas emissions estimation at country scale. J. Clean. Prod. 188, 851-859.
24. Liu, M., Yang, M., Chen, M., Yu, D., Zheng, J., Chang, J., Wang, X., Jie, C., Wei, Y. (2018). Numerical optimization of membrane module design and operation for a full-scale submerged MBR by computational fluid dynamics, Bioresource Technology 269, 300 – 308.
25. Maere, T., Verrecht, B., Moerenhout, S., Judd, S., Nopens, I. (2011). BSM-MBR: A benchmark simulation model to compare control and operational strategies for membrane bioreactors. Water Research 45, 2181–2190.
26. Maere, T., Verrecht, B., Moerenhout, S., Judd, S., Nopens, I. (2011). BSM-MBR: A benchmark simulation model to compare control and operational strategies for membrane bioreactors. Water Research 45, 2181–2190.
27. Mannina, G., Capodici, M., Cosenza, A., Di Trapani, D., 2016. Carbon and nutrient biological removal in a University of Cape Townmembrane bioreactor: Analysis of a pilot plant operated under twodifferent C/N ratios. Chemical Engineering Journal 296, 289–299.
28. Mannina, G., Cosenza, A. (2015). Quantifying sensitivity and uncertainty analysis of a new mathematical model for the evaluation of greenhouse gas emissions from membrane bioreactors. Journal of Membrane Science 475, 80–90.

29. Mannina, G., Cosenza, A., Ekama, G. (2018b). A comprehensive integrated membrane bioreactor model for greenhouse gas emissions. Chemical Engineering Journal, 334, 1563–1572.

30. Mannina, G., Cosenza, A., Viviani, G., Ekama, G. A. (2018a). Sensitivity and uncertainty analysis of an integrated ASM2d MBR model for wastewater treatment. Chemical Engineering Journal 351, 579–588.

31. Mannina, G., Rebouças, T.F., Cosenza, A., Olsson, G. (2019). Minimizing membrane bioreactor environmental footprint considering multiple objectives. In Proceedings of the 9th International Water Association (IWA) Membrane Technology Conference & Exhibition for Water and Wastewater Treatment and Reuse (IWA-MTC 2019); 23-27 June 2019 Toulouse, France.

32. Metcalf, & Eddy, Inc. 2003. Wastewater engineering: treatment and reuse. In: Tchobanoglous, G., Burton, F.L., Stensel, H.D. (Eds.), McGraw-Hill Series in Civil and Environmental Engineering, fourth ed. (New York).

33. Nopens, I., Benedetti, L., Jeppsson, U., Pons, M.-N., Alex, J., Copp, J.B., Gernaey, K.V., Rosen, C., Steyer, J.-P., Vanrolleghem, P.A. (2010). Benchmark simulation model no 2: finalisation of plant layout and default control strategy. Water Sci. Technol. 62 (9), 1967-1974.

34. Olsson, G., Newell, B. (1999). Wastewater Treatment System – Modelling, Diagnosis and Control. IWA Publishing, London.

35. Pocquet, M., Wu, Z., Queinnec, I., Spérandio, M. (2016). A two pathway model for N2O emissions by ammonium oxidizing bacteria supported by the NO/N2O variation. Water Res.88, 948-959.

36. Polruang, S., Sirivithayapakorn, S., Prateep, N. T. R. (2018). A comparative life cycle assessment of municipal wastewater treatment plants in Thailand under variable power schemes and effluent management programs. J. Clean. Prod. 172, 635-648.

37. Rivas, A., Irizar, I., Ayesa, E. (2008). Model-based optimization of wastewater treatment plants design, Environ. Modell. Softw. 23, 435–450.

38. Robles, A., Ruano, M.V., Charfi, A., Lesage, G., Heran, M., Harmand, J., Seco, A., Steyerd, J.-P., Batstone, D.J., Jeonghwan, K., Ferrer, J., (2018). A review on anaerobic membrane bioreactors (AnMBRs) focused on modelling and control aspects. Bioresource Technology 270, 612–626.

39. Robles, A., Ruano, M.V., Ribes, J., Seco, A., Ferrer, J. (2014). Model-based automatic tuning of a filtration control system for submerged anaerobic membrane bioreactors (AnMBR). Journal of Membrane Science 465, 14–26.

40. She, Q., Wang, R., Fane, A. G., Tang, C. Y. (2016). Membrane fouling in osmotically driven membrane processes: a review. J. Membr. Sci. 499, 201 - 233. Wazhab, N. A., Katebi, R., Balderub, J (2009). Multivariable PID control design for activated sludge process with nitrification and denitrification. Biochemical Engineering Journal 45 (3), 239 – 248.

41. Solon, K., Flores-Alsina, X., Kazadi Mbamba, C., Ikumi, D., Volcke, E.I.P., Vaneeckhaute, C., Ekama, G., Vanrolleghem, P.A., Batstone, D.J., Gernaey, K.V. (2017). Plant-wide modelling of phosphorus transformations in wastewater treatment systems: impacts of control and operational strategies. Water Research 113, 97-110.

42. Sun, J., Liang, P., Yan, X., Zuo, H., Xiao, K., Xia, J., Qiu, Y., Wu, Q., Wu, S., Huang, X., Qi, M., Wen, X. (2016). Reducing aeration energy consumption in a large-scale membrane bioreactor: process simulation and engineering application. Water Research 93, 205 – 213.

43. Sun, J., Liang, P., Yan, X., Zuo, K., Xiao, K., Xia, J., Qiu, Y., Wu, Q., Wu, S., Huang, X., Qi, M., Wen, X. (2016). Reducing aeration energy consumption in a large-scale membrane bioreactor: Process simulation and engineering application. Water Research 93, 205 – 213.

44. Tchobanoglous, G., Burton, F.L., Stensel, H.D. (2003). Wastewater Engineering: Treatment and Reuse. McGraw-Hill, Boston.

45. Vanrolleghem, P.A., Gillot, S. (2002). Robustness and economic measures as control benchmark performance criteria, Water Sci. Technol. 45 (4–5), 117–126.
46. Wallis-Lage, C. And Levesque, S. (2009). Cost effective and energy efficient MBR systems. In: Proceedings of Singapore International Water Week, 22–25 June, Singapore. Available from: http://bvwater.files.wordpress.com/2009/05/ abstract_siw09_wallis-lage.pdf.
47. Wu, Y., Xi, Y., Jing, X., Cai, P., Igalavithana, A. D., Tang, C., Tsang, D. C. W., Ok, Y. S. (2020). Recent advances in mitigating membrane biofouling using carbon-based materials. Journal of Hazardous Materials 382, 120976.
48. Xiao, K., Xu, Y., Liang, S., Lei, T., Sun, J., Wen, X., Zhang, H., Chen, C., Huang, X. (2014). Engineering application of membrane bioreactor for wastewater treatment in China: current state and future prospect. Front. Environ. Sci. Eng. 8, 805–819.
49. Yang, Y. Q., Zhan, X., Wu, S. J., Kang, M. L., Guo, J. A. (2016). Effect of hydraulic loading rate on pollutant removal efficiency in subsurface infiltration system under intermittent operation and micro-power aeration. Bioresource Technology 205, 174-182.
50. Zhang, M., Leung, K., H., Liao, B. (2019). Characterization of foaming and non-foaming sludge relating to aeration and the implications for membrane fouling control in submerged membrane bioreactors. Journal of Water Process Engineering 28, 250-259.